Rotationally Invariant Bark Recognition

Václav Remeš and Michal Haindl(✉)

The Institute of Information Theory and Automation,
Czech Academy of Sciences, Prague, Czech Republic
{remes,haindl}@utia.cz
http://www.utia.cz/

Abstract. An efficient bark recognition method based on a novel wide-sense Markov spiral model textural representation is presented. Unlike the alternative bark recognition methods based on various gray-scale discriminative textural descriptions, we benefit from fully descriptive color, rotationally invariant bark texture representation. The proposed method significantly outperforms the state-of-the-art bark recognition approaches in terms of the classification accuracy.

Keywords: Bark recognition · Tree taxonomy classification
Spiral Markov random field model

1 Introduction

Automatic bark recognition is a challenging but practical plant taxonomy application which allows fast and non-invasive tree recognition irrespective of the growing season, i.e., whether a tree has or has not its leaves, fruit, needles, or seeds or if the tree is healthy growing or just a dead stump. Automatic bark recognition makes identification or learning of tree species possible without any botanical expert knowledge through, e.g., using a dedicated mobile application. Manual identification of a tree's species based on a botanical key of bark images is a tedious task which would normally consist of scrolling through a book. Since bark can not be described as easily as leaves or needles [5,18], the user has to go through the whole bark encyclopedia looking for the corresponding bark image.

An advantage of bark based features is their relative stability during the corresponding tree's life time. Single shrubs or trees have specific bark which can be advantageously used for their identification. It enables numerous ecological applications such as plant resource management or fast identification of invading tree species. Industrial applications can be in saw mills or bark beetle tree infestation detection.

1.1 Alternative Bark Recognition Methods

A SVM type of classifier and gray-scale LBP features are used in [1]. Their dataset is a collection of 40 images per species and there are 23 species, i.e., a

X. Bai et al. (Eds.): S+SSPR 2018, LNCS 11004, pp. 22–31, 2018.
https://doi.org/10.1007/978-3-319-97785-0_3

total of 920 bark color images of local, mostly dry subtropical-climate, shrubs and trees (acacias, agaves, opuntias, palms). The classifier exploited in [9] is a radial basis probabilistic neural network. The method uses Daubechies 3rd level wavelet based features applied to each color band in the YC_bC_r color space. A similar method [8] with the same classifier uses Gabor wavelet features. Both methods use the same test set which contains 300 color bark images. Gabor banks features with a narrow-band signal model in 1-NN classifier was proposed in [4]. The test set has 8 species with 25 samples per tree category. The author also demonstrates a significant, but expectable, performance improvement when color information was added. The 1-NN and 4-NN classifier [19] represent bark textures by the run length, Haralick's co-occurrence matrix based, and histogram features. These methods are verified on a limited dataset of 160 samples from 9 species. Authors in [3] propose a rotationally invariant statistical radial binary pattern (SRBP) descriptor to characterize a bark texture. Four types of multi-scale LBP features (Multi-Block LBP (MBLBP) with a mean filter, LBP Filtering (LBPF), Multi-Scale LBP (MSLBP) with a low pass Gaussian filter, and Pyramid-based LBP (PLPB) with a pyramid transform) are used in [2]. Two bark image datasets (AFF [5], Trunk12 [17]) were used to evaluate the multi-scale LBP descriptors based bark recognition. The authors observed that multi-scale LBP provides more discriminative texture features than basic and uniform LBP and that LBPF gives the best results over all the tested descriptors on both datasets. The paper [15] proposes a combination of two types of texture features, the gray-level co-occurrence matrix metrics and the long connection length emphasis [15] binary texture features. Eighteen tree species in 90 images are classified using the k-NN classifier. The support vector machine classifier and multiscale rotationally invariant LBP features are used in [16]. The multi-class classification problem is solved using the one versus all scheme. The method is verified on two general texture datasets and the AFF bark dataset [5]. A comparison of the usefulness of the run-length method (5 features), co-occurrence correlation method (100) features for the bark k-NN classification into nine categories with 15 samples per category is presented in [19]. The method [5] uses support vector machine classifier with radial basis function kernel applied with four (contrast, correlation, homogeneity, and energy) gray-level co-occurrence matrices (GLCM), SIFT based bag-of-words, and wavelet features. The bark dataset (AFF bark dataset) consists of 1183 images of the eleven most common Austrian trees (Sect. 4). Color descriptor based on three-dimensional adaptive sum and difference histograms was applied BarTex textures in [13,14].

The majority of the published methods suffer from neglecting spectral information and using discriminative and thus approximate textural features only. Few attempts to use multispectral information [8,9,11,19] independently apply monospectral features on each spectral band or apply the color LBP features [7,12]. Most methods use private and very restricted bark databases, thus the published results are mutually incomparable and of limited information value.

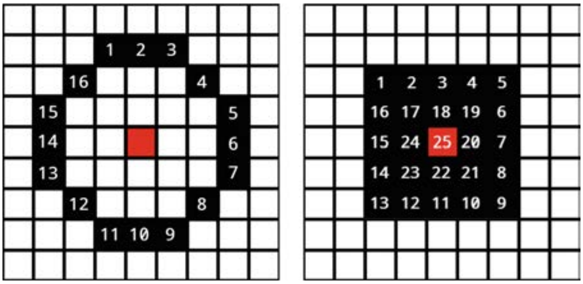

Fig. 1. The paths of the two "spirals" in an image. Left: octagonal, right: rectangular. The numbers designate the order in which the pixels r, i.e., I_r^{cs} neighborhoods are traversed and the red square means the center pixel. (Color figure online)

2 Spiral Markovian Texture Representation

The spiral adaptive 2D causal auto-regressive random (2DSCAR) field model is a generalization of the 2DCAR model [6]. The model's functional contextual neighbour index shift set is denoted I_r^{cs}. The model can be defined in the following matrix equation:

$$Y_r = \gamma Z_r + e_r, \tag{1}$$

where $\gamma = [a_1, \ldots, a_\eta]$ is the parameter vector, $\eta = \mathit{cardinality}(I_r^{cs})$, $r = [r_1, r_2]$ is spatial index denoting history of movements on the lattice I, e_r denotes driving white Gaussian noise with zero mean and a constant but unknown variance σ^2, and Z_r is a neighborhood support vector of Y_{r-s} where $s \in I_r^{cs}$.

All 2DSCAR model statistics can be efficiently estimated analytically [6]. The Bayesian parameter estimation (conditional mean value) $\hat{\gamma}$ can be accomplished using fast, numerically robust and recursive statistics [6], given the known 2DSCAR process history $Y^{(t-1)} = \{Y_{t-1}, Y_{t-2}, \ldots, Y_1, Z_t, Z_{t-1}, \ldots, Z_1\}$:

$$\hat{\gamma}_{t-1}^T = V_{zz(t-1)}^{-1} V_{zy(t-1)}, \tag{2}$$

$$V_{t-1} = \tilde{V}_{t-1} + V_0, \tag{3}$$

$$\tilde{V}_{t-1} = \begin{pmatrix} \sum_{u=1}^{t-1} Y_u Y_u^T & \sum_{u=1}^{t-1} Y_u Z_u^T \\ \sum_{u=1}^{t-1} Z_u Y_u^T & \sum_{u=1}^{t-1} Z_u Z_u^T \end{pmatrix} = \begin{pmatrix} \tilde{V}_{yy(t-1)} & \tilde{V}_{zy(t-1)}^T \\ \tilde{V}_{zy(t-1)} & \tilde{V}_{zz(t-1)} \end{pmatrix}, \tag{4}$$

where t is the traversing order index of the sequence of multi-indices, r is based on the selected model movement in the lattice I (see Fig. 1), V_0 is a positive definite initialization matrix (see [6]). The optimal causal functional contextual neighbourhood I_r^{cs} can be solved analytically by a straightforward generalisation of the Bayesian estimate in [6]. The model can be easily applied also to numerous synthesis applications. The 2DSCAR model pixel-wise synthesis is simple direct application of (1) for any 2DSCAR model.

2.1 Spiral Models

The 2DSCAR model's movement r on the lattice I takes the form of circular or spiral like paths as seen in Fig. 1. The causal neighborhood I_r^c has to be transformed to be consistent for each direction in the traversed path to. The paths used can be arbitrary as long as they keep transforming the causal neighborhood into I_r^{cs} in such a way that all neighbors of a control pixel r have been visited by the model in the previous steps. We shall call all these paths as spirals further on. We present two types of paths - octagonal (Fig. 1 on the left) and a rectangular spiral (Fig. 1 - right). During our experiments they exhibited comparable results with the octagonal path being faster thanks to its consisting of fewer pixels for the same radius.

After the whole path is traversed, the parameters for the center pixel (shown as red square in Fig. 1) of the spiral are estimated. Contrary to the standard CAR model [6], since this model's equations do not need the whole history of movement through the image but only the given one spiral, the 2DSCAR models can be easily parallelized. If the spiral paths used have circular shape, the 2DSCAR models exhibit rotational invariant properties thanks to the CAR model's memory of all the visited pixels. The spiral neighborhood I_r^{cs} (Fig. 1 - right) is rotationally invariant only approximately. Additional contextual information can be easily incorporated if every initialization matrix $V_0 = V_{t-1}$, i.e., if this matrix is initialized from the previous data gathering matrix.

Fig. 2. Examples of images from the individual datasets. Top to bottom (rightwards): AFF (ash, black pine, fir, hornbeam, larch, mountain oak, Scots pine, spruce, Swiss stone pine, sycamore maple, beech), BarkTex (betula pendula, fagus silvatica, picea abies, pinus silvestris, quercus robur, robinia pseudacacia), Trunk12 (alder, beech, birch, ginkgo biloba, hornbeam, horse chestnut, chestnut, linden, oak, oriental plane, pine, spruce).

2.2 Feature Extraction

For feature extraction, we analyzed the 2DSCAR model around pixels in each spectral band with vertical and horizontal stride of 2 to speed up the computation. The following illumination invariant features originally derived for the

2DCAR model [6] were adapted for the 2DSCAR:

$$\alpha_1 = 1 + Z_r^T V_{zz}^{-1} Z_r, \tag{5}$$

$$\alpha_2 = \sqrt{\sum_r \left(Y_r - \hat{\gamma} Z_r\right)^T \lambda_r^{-1} \left(Y_r - \hat{\gamma} Z_r\right)}, \tag{6}$$

$$\alpha_3 = \sqrt{\sum_r \left(Y_r - \mu\right)^T \lambda_r^{-1} \left(Y_r - \mu\right)}, \tag{7}$$

where μ is the mean value of vector Y_r and

$$\lambda_{t-1} = V_{yy(t-1)} - V_{zy(t-1)}^T V_{zz(t-1)}^{-1}.$$

As the texture features, we also used the estimated γ parameters, the posterior probability density [6]

$$p(Y_r | Y^{(r-1)}, \hat{\gamma}_{r-1}) = \frac{\Gamma(\frac{\beta(r)-\eta+3}{2})}{\Gamma(\frac{\beta(r)-\eta+2}{2})\ \pi^{\frac{1}{2}}\ \left(1 + X_r^T V_{x(r-1)}^{-1} X_r\right)^{\frac{1}{2}}\ |\lambda_{(r-1)}|^{\frac{1}{2}}}$$
$$\left(1 + \frac{(Y_r - \hat{\gamma}_{r-1} X_r)^T \lambda_{(r-1)}^{-1} (Y_r - \hat{\gamma}_{r-1} X_r)}{1 + X_r^T V_{x(r-1)}^{-1} X_r}\right)^{-\frac{\beta(r)-\eta+3}{2}}, \tag{8}$$

and the absolute error of the one-step-ahead prediction

$$Abs(GE) = \left| E\left\{ Y_r | Y^{(r-1)} \right\} - Y_r \right| = \left| Y_r - \hat{\gamma}_{r-1} X_r \right|. \tag{9}$$

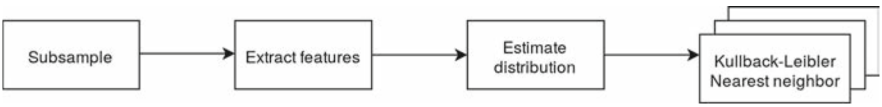

Fig. 3. Flowchart of our classification approach.

3 Bark Texture Recognition

To speed up the feature extraction part, we first subsample the images to the height of 300px (if the image is larger), keeping aspect ratio. This subsampling ratio depends on an application data, i.e., a compromise between the algorithm efficiency and its recognition rate. The features are then extracted as described in Sect. 2. The feature space is assumed to be approximated by the multivariate Gaussian distribution, the parameters of which are then stored for each training sample image.

$$\mathcal{N}(\theta|\mu,\Sigma)=\frac{1}{\sqrt{(2\pi)^N|\Sigma|}}e^{\left(-\frac{1}{2}(\theta-\mu)^{\mathrm{T}}\Sigma^{-1}(\theta-\mu)\right)}.$$

During the classification stage, the parameters of the Gaussian distribution are estimated for the classified image as in the training step (the flowchart of our approach can be seen in Fig. 3). They are then compared with all the distributions of the training samples using the Kullback-Leibler (KL) divergence. The KL divergence is a measure of how much one probability distribution diverges from another. It is defined as:

$$D(f(x)||g(x))\stackrel{def}{=}\int f(x)\log\frac{f(x)}{g(x)}\,dx\,.$$

For the Gaussian distribution data model, the KL divergence can be solved analytically:

$$D(f(x)||g(x))=\frac{1}{2}\left(\log\frac{|\Sigma_g|}{|\Sigma_f|}+tr(\Sigma_g^{-1}\Sigma_f)-d+(\mu_f-\mu_g)^T\Sigma_g^{-1}(\mu_f-\mu_g)\right).$$

We use the symmetrized variant of the Kullback-Leibler divergence known as the Jeffreys divergence

$$D_s(f(x)||g(x))=\frac{D(f(x)||g(x))+D(g(x)||f(x))}{2}.$$

The class of the training sample with the lowest divergence from the image being recognized is then selected as the final result. The advantage of our approach is that the training database is heavily compressed through the Gaussian distribution parameters (as we extract only about 40 features, depending on the chosen neighborhood, we only need to store 40 numbers for the mean and 40×40 numbers for the covariance matrix) and the comparison with the training database is extremely fast, enabling us to compare hundreds of thousands of image feature distributions per second on an ordinary computer.

4 Experimental Results

The proposed method is verified on three publicly available bark databases and our own bark dataset (not demonstrated here). Examples of images of the datasets can be seen in Fig. 2. We have used the leave-one-out approach for the classification rate estimation.

The AFF bark dataset provided by Osterreichische Bundesforste, Austrian Federal Forests (AFF) [5], is a collection of the most common Austrian trees. The dataset contains 1182 bark samples belonging to 11 classes, the size of each class varying between 7 and 213 images. AFF samples are captured at different scales, and under different illumination conditions.

The Trunk12 dataset ([17], http://www.vicos.si/Downloads/TRUNK12) contains 393 images of tree barks belonging to 12 different trees that are found in Slovenia. The number of images per class varies between 30 and 45 images.

Table 1. AFF bark dataset results of the presented method (MO - Mountain oak, SP - Scots pine, SSP - Swiss stone pine, SM - Sycamore maple).

	Ash	Beech	Black pine	Fir	Horn-beam	Larch	MO	SP	Spruce	SSP	SM	Sensitivity [%]
Ash	22	0	0	1	0	0	0	0	0	0	1	91.7
Beech	0	7	0	0	0	0	0	0	0	0	0	100
B. pine	0	0	139	0	0	9	0	8	0	1	0	88.5
Fir	0	0	0	105	0	6	0	5	2	0	0	89.0
Horn.	0	0	1	0	32	0	0	0	0	0	0	97.0
Larch	0	0	6	0	0	156	0	27	0	2	0	81.7
MO	0	0	0	0	0	1	59	0	3	5	0	86.8
SP	0	0	9	1	0	28	0	142	1	0	0	78.5
Spruce	1	0	3	4	0	6	2	4	181	3	0	88.7
SSP	0	0	5	2	0	7	9	0	4	60	0	69.0
SM	1	0	0	0	3	0	3	0	0	3	2	16.7
Precision [%]	91.7	100	85.3	92.9	91.4	73.2	80.8	76.3	94.8	81.1	66.7	**Accuracy 83.6**

Bark images are captured under controlled scale, illumination and pose conditions. The classes are more homogeneous than those of AFF in terms of imaging conditions.

The BarkTex dataset [10] contains 408 samples from 6 bark classes, i.e., 68 images per class. The images have small (256×384) resolution and they have unequal natural illumination and scale.

We have achieved the accuracy of 83.6% on the AFF dataset (Table 1), 91.7% on the BarkTex database (Table 2) and 92.9% on the Trunk12 dataset (Table 3). In all the three tables, the name of the row indicates the actual tree type whereas the column indicates the predicted class. The comparison with other methods

Table 2. BarkTex dataset results of the presented method (BP - Betula pendula, FS - Fagus silvatica, PA - Picea abies, PS - Pinus silvestris, QR - Quercus robur, RP - Robinia pseudacacia).

	BP	FS	PA	PS	QR	RP	Sensitivity [%]
Betula pendula	64	0	0	2	2	0	94.1
Fagus silvatica	0	68	0	0	0	0	100.0
Picea abies	3	0	62	0	3	0	91.2
Pinus silvestris	0	0	1	67	0	0	98.5
Quercus robur	1	2	7	9	48	1	70.6
Robinia pseudacacia	1	0	0	1	1	65	95.6
Precision [%]	92.8	97.1	88.6	84.8	88.9	98.5	**Accuracy 91.7**

Table 3. Trunk12 dataset results of the presented method (A - Alder, Be - Beech, Bi - Birch, Ch - Chestnut, GB - Ginkgo biloba, H - Hornbeam, HC - Horse chestnut, L - Linden, OP - Oriental plane, S - Spruce).

	A	Be	Bi	Ch	GB	H	HC	L	Oak	OP	Pine	S	Sensitivity [%]
Alder	33	0	1	0	0	0	0	0	0	0	0	0	97.1
Beech	0	29	0	0	0	1	0	0	0	0	0	0	96.7
Birch	0	0	36	1	0	0	0	0	0	0	0	0	97.3
Chestnut	2	0	0	24	0	0	0	0	4	0	2	0	75.0
Ginkgo biloba	0	0	0	0	30	0	0	0	0	0	0	0	100
Hornbeam	0	2	0	0	0	28	0	0	0	0	0	0	93.3
Horse chestnut	0	0	1	0	0	1	27	3	0	0	1	0	81.8
Linden	0	0	0	1	0	0	4	25	0	0	0	0	83.3
Oak	1	0	0	0	0	0	0	0	29	0	0	0	96.7
Oriental plane	0	0	0	1	0	0	1	0	0	30	0	0	93.8
Pine	0	0	0	0	0	0	0	0	0	0	30	0	100
Spruce	1	0	0	0	0	0	0	0	0	0	0	44	97.8
Precision [%]	89.2	93.5	94.7	88.9	100	93.3	84.4	89.3	87.9	100	90.9	100	**Accuracy 92.9**

Table 4. Comparison with the state-of-the-art. ‘x’ denotes lack of results in the particular article on the given dataset.

Dataset [%]	Our results	[3]	[5]	[16]	[7]	[11]	[12]	[14]	[13]
AFF	83.6	60.5	69.7	**96.5**	-	-	-	-	-
BarkTex	**91.7**	84.6	-	-	81.4	84.7	81.4	82.1	89.6
Trunk12	**92.9**	62.8	-	-	-	-	-	-	-

is presented in Table 4. We can see that our approach vastly outperforms all compared methods on the BarkTex and Trunk12 datasets and has the second best results on the AFF dataset.

5 Conclusion

The presented tree bark recognition method uses an underlying descriptive textural model for the classification features and outperforms the state-of-the-art alternative methods on two public bark databases and is the second best on the AFF database. Our method is rotationally invariant, benefits from information from all spectral bands and can be easily parallelized or made fully illumination invariant. We have also executed our method without any modification on the AFF dataset's images of needles and leaves, with results exceeding 94% accuracy. This will be a subject of our further research.

References

1. Blaanco, L.J., Travieso, C.M., Quinteiro, J.M., Hernandez, P.V., Dutta, M.K., Singh, A.: A bark recognition algorithm for plant classification using a least square support vector machine. In: 2016 Ninth International Conference on Contemporary Computing, IC3, pp. 1–5, August 2016. https://doi.org/10.1109/IC3.2016.7880233
2. Boudra, S., Yahiaoui, I., Behloul, A.: A comparison of multi-scale local binary pattern variants for bark image retrieval. In: Battiato, S., Blanc-Talon, J., Gallo, G., Philips, W., Popescu, D., Scheunders, P. (eds.) ACIVS 2015. LNCS, vol. 9386, pp. 764–775. Springer, Cham (2015). https://doi.org/10.1007/978-3-319-25903-1_66
3. Boudra, S., Yahiaoui, I., Behloul, A.: Statistical radial binary patterns (SRBP) for bark texture identification. In: Blanc-Talon, J., Penne, R., Philips, W., Popescu, D., Scheunders, P. (eds.) ACIVS 2017. LNCS, vol. 10617, pp. 101–113. Springer, Cham (2017). https://doi.org/10.1007/978-3-319-70353-4_9
4. Chi, Z., Houqiang, L., Chao, W.: Plant species recognition based on bark patterns using novel Gabor filter banks. In: Proceedings of the 2003 International Conference on Neural Networks and Signal Processing, vol. 2, pp. 1035–1038, December 2003. https://doi.org/10.1109/ICNNSP.2003.1281045
5. Fiel, S., Sablatnig, R.: Automated identification of tree species from images of the bark, leaves and needles. In: 16th Computer Vision Winter Workshop, pp. 67–74. Verlag der Technischen Universität Graz (2011)
6. Haindl, M.: Visual data recognition and modeling based on local Markovian models. In: Florack, L., Duits, R., Jongbloed, G., van Lieshout, M.C., Davies, L. (eds.) Mathematical Methods for Signal and Image Analysis and Representation. CIVI, vol. 41, pp. 241–259. Springer, London (2012). https://doi.org/10.1007/978-1-4471-2353-8_14
7. Hoang, V.T., Porebski, A., Vandenbroucke, N., Hamad, D.: LBP histogram selection based on sparse representation for color texture classification. In: VISIGRAPP (4: VISAPP), pp. 476–483 (2017)
8. Huang, Z.K.: Bark classification using RBPNN based on both color and texture feature. Int. J. Comput. Sci. Netw. Secur. **6**(10), 100–103 (2006)
9. Huang, Z.K., Huang, D.S., Lyu, M.R., Lok, T.M.: Classification based on Gabor filter using RBPNN classification. In: 2006 International Conference on Computational Intelligence and Security, vol. 1, pp. 759–762. IEEE (2006)
10. Lakmann, R.: Statistische Modellierung von Farbtexturen. Ph.D. thesis (1998). ftp://ftphost.uni-koblenz.de/de/ftp/pub/outgoing/vision/Lakman/BarkTex/
11. Palm, C.: Color texture classification by integrative co-occurrence matrices. Pattern Recognit. **37**(5), 965–976 (2004)
12. Porebski, A., Vandenbroucke, N., Hamad, D.: LBP histogram selection for supervised color texture classification. In: ICIP, pp. 3239–3243 (2013)
13. Sandi, F., Douik, A.: Dominant and minor sum and difference histograms for texture description. In: 2016 International Image Processing, Applications and Systems, IPAS, pp. 1–5, November 2016. https://doi.org/10.1109/IPAS.2016.7880136/
14. Sandid, F., Douik, A.: Robust color texture descriptor for material recognition. Pattern Recognit. Lett. **80**, 15–23 (2016). https://doi.org/10.1016/j.patrec.2016.05.010. http://www.sciencedirect.com/science/article/pii/S0167865516300885
15. Song, J., Chi, Z., Liu, J., Fu, H.: Bark classification by combining grayscale and binary texture features. In: Proceedings of 2004 International Symposium on Intelligent Multimedia, Video and Speech Processing, pp. 450–453. IEEE (2004)

16. Sulc, M., Matas, J.: Kernel-mapped histograms of multi-scale LBPs for tree bark recognition. In: 2013 28th International Conference of Image and Vision Computing New Zealand, IVCNZ, pp. 82–87. IEEE (2013)
17. Švab, M.: Computer-vision-based tree trunk recognition (2014)
18. Wäldchen, J., Mäder, P.: Plant species identification using computer vision techniques: a systematic literature review. Arch. Comput. Methods Eng. **25**(2), 507–543 (2018). https://doi.org/10.1007/s11831-016-9206-z
19. Wan, Y.Y., et al.: Bark texture feature extraction based on statistical texture analysis. In: Proceedings of 2004 International Symposium on Intelligent Multimedia, Video and Speech Processing, pp. 482–485, October 2004. https://doi.org/10.1109/ISIMP.2004.1434106